recombination of interstitial ions and vacancies is less pronounced, leading to a concentration of interstitial ions that increases rapidly with field.

3. Above a field of about 6×10^6 volts/cm, the position of the activation barrier for interstitial ion formation moves discontinuously to a position near the origin of the ion, and the field dependencies of the activation energies for creation and recombination become more nearly equal, so that the concentration of interstitial ions becomes less dependent upon field.

4. The influence of an electric field on the activation energy for ionic conductivity is twice as great at fields below 6×10^6 volts/cm as above, because at low fields both the number of charge carriers and their mobility is increasing with field, whereas above 6×10^6 volts/cm it is primarily their mobility that continues to increase.

PHYSICAL REVIEW VOLUME 101, NUMBER 2 JANUARY 15, 1956

Angular Dependence of the Characteristic Energy Loss of Electrons Passing Through Metal Foils*

RICHARD A. FERRELL
University of Maryland, College Park, Maryland
(Received August 3, 1955)

The Bohm-Pines electron plasma theory is employed to give a theoretical interpretation of some experimental results of Marton *et al.* on the scattering of 20-kev electrons by a thin gold foil. General criteria are presented which can in principle select in any given case between the alternative mechanisms of collective excitation or one-electron excitation. For the general case of collective excitation the scattering law is derived and used in a numerical analysis of the experimental data. Agreement with the Bohm-Pines theory is satisfactory.

I. INTRODUCTION

THE Franck-Hertz phenomenon in gases has long provided a tool, along with optical spectroscopy, for investigating the electronic energy level structure in gaseous atoms and molecules. The corresponding phenomenon in solids, because of technical difficulties, has been exploited more slowly. Rudberg[1] seems to be the first to have noticed that electrons of a few hundred volts, when reflected from solid samples of the noble metals, preferentially lose amounts of energy characteristic of the target metal. In each of these metals Rudberg found two characteristic energy losses, which we for short call "eigenlosses," all less than ten volts. Rudberg and Slater[2] interpreted these eigenlosses as one-electron interband transitions in which electrons occupying the filled d-band were excited to the top of the $s-p$ band, thereby absorbing energy from and inelastically scattering the incident electrons. The discreteness of the loss spectrum arises from the "double-humped" character of the density of states curve for the filled d-band. There can be little doubt of the correctness of this interpretation, for it not only rests on some quite basic features of the band theory, but is also supported by the close correlation between the eigenlosses of Rudberg and the optical absorption peaks determined independently by Minor, and Meier.[3] For example, the absorption of gold in the blue, which causes its reddish color, has a maximum at 3700 A, corresponding to a quantum energy of 3.36 ev. This agrees well with Rudberg's 3-volt eigenloss. Since the optical absorption is also due to the same mechanism of excitation of the d-band electrons, this agreement is necessary. In general, the hypothesis that a given eigenloss is a one-electron interband transition can be tested by examining the optical absorption data. If there is no absorption for light of quantum energy equal to the eigenloss, the interband hypothesis must be rejected in the specific case at hand.

Unfortunately, the optical absorption data are not very complete and it is not possible in practice to apply this test in very many cases. As already mentioned, Rudberg's low-energy eigenlosses for the noble metals pass the test. On the other hand, many eigenlosses discovered since Rudberg's early experiments do not satisfy this criterion. For example, there are no optical absorptions corresponding to the eigenlosses found by Marton and Leder[4] for the alkali metals. In such cases the one-electron hypothesis must be abandoned in favor of a collective excitation involving the totality of the electrons in the metal. Collective phenomena lie outside the scope of the usual one-electron theory of metals, but are included from the start in the Bohm-Pines[5] plasma theory of the free-electron gas. Modifications to take into account the interaction of the conduction electrons with the more tightly bound

* Research supported by the Office of Naval Research.
[1] E. Rudberg, Phys. Rev. **50**, 138 (1936).
[2] E. Rudberg and J. C. Slater, Phys. Rev. **50**, 150 (1936).
[3] R. S. Minor, Ann. Physik **10**, 581 (1903), and W. Meier, Ann. Physik **31**, 1017 (1910).
[4] L. Marton and Lewis B. Leder, Phys. Rev. **94**, 203 (1954).
[5] D. Bohm and D. Pines, Phys. Rev. **92**, 609 (1953), and David Pines, Phys. Rev. **92**, 626 (1953).

electrons and with the positive ion lattice have been established by Wolff[6] and Hubbard.[7]

Multiple scattering is an inherent complication in the reflection-type inelastic scattering experiments of Rudberg. Therefore transmission-type experiments are preferable and easier to interpret theoretically, provided the incident electrons are fast enough and the samples are thin enough that the relative intensity of the singly scattered component of the emerging inelastic beam is large compared to that of the multiply scattered component. Using electrons of a few kev energy and metal foils of a few hundred angstrom units thickness, Ruthemann[8] discovered prominent eigenlosses in the energy range of 10 to 30 volts for several metals. Since Ruthemann's discovery, experimental data have been rapidly accumulated by many investigators.[9] Many of the prominent (i.e., high intensity) eigenlosses of considerable energy have been successfully interpreted by the Bohm-Pines free-electron theory. The most familiar cases are the 14.7-ev loss in aluminum and the 18.9-ev loss in beryllium. Other cases seem to require the effective-mass modification of the Bohm-Pines theory mentioned above. There has been considerable controversy on the question of whether Bohm-Pines theory or one-electron theory is the correct explanation of the eigenlosses in metals. We advocate here the view that in general in every metal there will be one collective eigenloss of relatively large energy and intensity, and, in addition, from none to several one-electron eigenlosses of generally smaller energy and intensity. Thus, both mechanisms can operate in the same metal. Corresponding to the comparison of one-electron eigenlosses with optical absorption peaks there is also a test for the collective eigenlosses. They must agree with the quantum energy of the cut-off radiation . . . , i.e., the lowest frequency electromagnetic radiation transmitted by the metal. This criterion is discussed more fully in Sec. II.

Recently information has been obtained on the angular dependence of the eigenlosses. Watanabe[10] has investigated the dependence of the loss energy as a function of scattering angle, and has found good agreement in aluminum and beryllium with the Bohm-Pines dispersion law for the plasma oscillations.[5] Other measurements by Leonhard[11] and by Marton, Simpson, and McCraw[12] have been especially suited for a study of the intensity of the eigenlosses in various metals. The principal purpose of this paper is to give a theoretical interpretation of these latter experimental results. Because of the completeness of the experimental data for gold, we shall concentrate on the 24-ev eigenloss in this metal. This latter eigenloss was already indicated by the results of Rudberg[1] and shows up especially clearly in the transmission experiments. Because of its large energy, this eigenloss probably lies well above the main electromagnetic absorptions, and therefore is unlikely to be a result of one-electron interband transitions. This is, of course, by no means well established, since the optical data do not extend below wavelengths of 2000 A, or above quantum energies of about six electron volts. In any case, our present work rests on the assumption that this eigenloss is not due to one-electron jumps, but rather to a Bohm-Pines collective excitation of the electron plasma. If this assumption is incorrect, a detailed analysis of the band transitions would have to be made, similar to the work of Rudberg and Slater on the lower energy eigenlosses.

Since the angular dependences of the matrix elements for collective excitation and interband one-electron excitation happen to agree in first approximation, it is likely that the intensity angular defendence predicted on the basis of one-electron theory will not differ greatly from that found here.[13] For this reason the intensity angular dependence should not be relied upon to distinguish between the two alternative mechanisms. The choice should be based on other criteria, such as the optical absorption test and optical transmission test discussed here and in Sec. II, the angular dependence of the magnitude of the eigenloss energy mentioned above, independent information on the band structure, etc. In the present work, having made our choice, we wish to show merely that the observed angular dependence is not inconsistent with it (*viz.*, the hypothesis of plasma excitation).

In Part II, as well as discussing a general criterion for collective excitation, we derive, on the basis of Bohm-Pines theory, the intensity angular dependence of the inelastically scattered electrons. This is supplemented by a study in Part III of the one-electron transitions which occur for collision distances shorter than the Bohm-Pines screening length. Unfortunately these consequences of the Bohm-Pines theory cannot be compared directly with experiment because of elastic scattering by the positive-ion lattice. This complication is treated in general in Part IV, where also the results of numerical calculation are presented, and satisfactory agreement with experiment is exhibited in Fig. 3.

II. BOHM-PINES THEORY

The original unmodified theory of Bohm and Pines[5] applies only to a free electron gas. In a real metal it is necessary to include not only the effective mass cor-

[6] P. Wolff, Phys. Rev. **92**, 18 (1953).
[7] J. Hubbard, Proc. Phys. Soc. (London) **A67**, 1058 (1954).
[8] G. Ruthemann, Ann. Physik **6**, **2**, 113 (1948).
[9] See reference 4 and also the forthcoming review: Marton, Leder, and Mendlowitz, *Advances in Electronics and Electron Physics* (Academic Press, Inc., New York, 1954), Vol. 6.
[10] H. Watanabe, J. Phys. Soc. Japan **10**, 321 (1955), and private communication.
[11] F. Leonhard, Z. Naturforsch. **9a**, 727 (1954), and **9a**, 1019 (1954).
[12] Marton, Simpson, and McCraw, Phys. Rev. **99**, 495 (1955).
[13] The author is greatly indebted to Dr. U. Fano for bringing this fact to his attention, by pointing out that the statement of the author [Phys. Rev. **99**, 647(A) (1955)] concerning the difference between plasma excitation and atomic excitation is incorrect.

rection mentioned above,[6,7] but also to take into account the virtual one-electron band transitions which can take place. A quantum-mechanical treatment of this problem has been given by Adams[14] but it will be sufficient to adopt here a semiclassical approach, developed by Mott.[15,16] We represent the virtual transitions by oscillators of natural frequency ω_i and strength f_i per atom. Let the displacement of the ith type oscillators, averaged over a region large compared to the interatomic spacing, be $\mathbf{y}_i(\mathbf{x})$, where $\mathbf{x}$ locates the region. Similarly, let the average electric field strength in the neighborhood of $\mathbf{x}$ be $\mathbf{E}(\mathbf{x})$. Then the oscillator displacements satisfy the equations of motion

$$\frac{d^2\mathbf{y}_i}{dt^2}+\omega_i^2\mathbf{y}_i=-\frac{e}{m}\mathbf{E}. \tag{1}$$

Similarly, the average displacement, $\mathbf{y}(\mathbf{x})$, of the conduction electrons satisfies the equation

$$\frac{d^2\mathbf{y}}{dt^2}=-\frac{e}{m^*}\mathbf{E}, \tag{2}$$

where $1/m^*$ is the reciprocal of the effective mass averaged over the Fermi sea. Now it is easily seen that the average charge density resulting from the displacements of the oscillator and conduction electrons is $ne(z\nabla\cdot\mathbf{y}+\sum_i f_i\nabla\cdot\mathbf{y}_i)$, and Poisson's equation therefore reads

$$4\pi nze\nabla\cdot\mathbf{y}+4\pi ne\textstyle\sum_i f_i\nabla\cdot\mathbf{y}_i=\nabla\cdot\mathbf{E}, \tag{3}$$

where n is the atomic density and z is the number of conduction electrons per atom. Taking the divergence of Eqs. (1) and (2) gives a set of simultaneous homogeneous linear equations in the unknowns $\nabla\cdot\mathbf{E}$, $\nabla\cdot\mathbf{y}$, and $\nabla\cdot\mathbf{y}_i$. Elimination of the latter leads to an ordinary homogeneous differential equation for $\nabla\cdot\mathbf{E}$ alone, whose solutions are harmonic oscillations in time, at the frequencies ω given by the roots of the equation

$$1+4\pi\left[\frac{nze^2}{m^*}\cdot\frac{1}{-\omega^2}+\frac{ne^2}{m}\sum_i\frac{f_i}{-\omega^2+\omega_i^2}\right]=0. \tag{4}$$

Oscillator damping may be expected to so smear out the singularities of the second term of the bracketed expression in Eq. (4) that, instead of many roots, there will be only one. This value of ω we identify with the single strong collective eigenloss identified unambiguously in most metals. In case the ω_i are all small relative to ω, the sum rule reduces (4) to

$$1-\frac{4\pi ne^2}{\omega^2 m}\left[z\frac{m}{m^*}+\sum_i f_i\right]=1-\frac{4\pi nz'e^2}{\omega^2 m}=0,$$

or to $\omega=(4\pi nz'e^2/m)^{\frac{1}{2}}$, where z' is the total number of electrons per atom. The quantity $(4\pi nz'e^2/m)^{\frac{1}{2}}$ is the free electron plasma frequency calculated on the basis of an electron density of nz', and denoting it by ω_p', we have $\omega=\omega_p'$. This result follows immediately in this special case when one neglects the binding and treats all the electrons as free. Actually, in gold all except the $6s$ and $5d$ electrons are tightly bound by several Rydbergs or more, and only the eleven electrons per atom in these two bands are available for participation in the collective oscillations. Thus we can consider ω_p', calculated with $z'=11$, as an upper limit for the value of ω. On the other hand, in case the ω_i are all very large relative to ω, the second term in the bracket of (4) may be neglected, yielding $\omega=(m/m^*)^{\frac{1}{2}}\omega_p$, where $\omega_p=(4\pi nze^2/m)^{\frac{1}{2}}$ is the free electron plasma frequency calculated on the basis of the density of conduction electrons alone. Consequently, the two limiting cases give us the inequalities

$$(\omega_p'/\omega_p)^2=11\geq(\omega/\omega_p)^2\geq m/m^*.$$

Now, taking the experimental data for gold, we find $(\omega/\omega_p)^2=6.9$. Since it is unlikely for m/m^* to be this large, the inequalities are satisfied. We conclude that gold represents a case intermediate between the two extreme cases discussed, and that in addition to being modified by interaction with the lattice, the plasma frequency is "pushed up" to some extent by the optical absorptions below it. This is an effect which has already been discovered by Wolff[6] in his investigations on shifts in the plasma frequency.

Although a quantitative solution of (4) is handicapped by insufficient theoretical and empirical knowledge of the energy bands, and is not in general feasible, there does exist an independent determination of the root ω. The bracketed term in (4) is identical with the polarizability of the metal, and the left-hand member itself expresses the dielectric constant of the metal as a function of frequency.[17] As ω is decreased from a very large value, the dielectric constant eventually becomes negative and the metal becomes perfectly reflecting. Thus the root of Eq. (4) is simply the cut-off minimum frequency for transmission of electromagnetic radiation through the metal. This furnishes the test already mentioned above which the hypothesis of collective excitation must satisfy: The eigenloss must correspond to the independently determined electromagnetic cut-off frequency.

Unfortunately, the electromagnetic data are, also for this test, too scarce for a systematic check of all the supposed collective eigenlosses. Only for the alkali

[14] E. N. Adams, Phys. Rev. **98**, 947 (1955).
[15] N. F. Mott, Proceedings of the Tenth Solvay Congress, Brussels, Belgium (1954).
[16] We are much indebted to Professor David Pines for bringing this approach to our attention. For more complete discussion of the frequency of plasma oscillations in solids, see D. Pines, Proceedings of the Tenth Solvay Congress, Brussels, Belgium (1954) and a review article by D. Pines which is to appear in *Advances in Solid State Physics* (Academic Press, Inc., New York, 1955), Vol. 1.
[17] F. Seitz, *The Modern Theory of Solids* (McGraw-Hill Book Company, Inc., New York, 1940), Chap. XVII.

TABLE I. Eigenlosses and cut-off quantum energies of the alkali metals.

Metal	Cutoff wavelength (in A)	Cutoff energy (in ev)	Eigenloss (in ev)	$\hbar\omega_p$ (in ev)
Li	1550	8.02	9.5±1.0	8.13
Na	2100	5.91	5.4±0.4	5.95
K	3150	3.94	3.8±0.2	4.38
*R*6	3400	3.65	···	3.97
Cs	3800	3.27	···	3.55

metals does a detailed comparison seem to be possible at the present time. Table I has been constructed from data of reference 4 and from page 641 of reference 17. The Bohm-Pines free electron plasma energies, $\hbar\omega_p$, are included for comparison. Bearing in mind that the influences both of the backing and of the oxide coatings on the measurements of the alkali metal eigenlosses are not completely determined, we may regard the agreement between the cut-off energies and the eigenlosses, where the latter have been measured, as satisfactory. The cut-off frequency in aluminum evidently has never been measured, but the metal is known to be perfectly reflecting far into the ultraviolet. On the basis of the sharp eigenloss at 14.7 ev, we can predict that aluminum will show an abrupt decrease in its reflectivity at 845 A. The electromagnetic properties of the other metals seem to be even less well known. If the absorptions should extend up to the plasma frequency, as is probably the case in gold, the transition from imperfect reflection to imperfect transmission can be expected to occur more gradually, corresponding to the greater breadth of the eigenloss. A verification of these features in aluminum and gold, as well as in other metals, would substantiate the hypothesis of collective excitation in each case individually.

After these general remarks on the Bohm-Pines theory, we now study the phenomenon of plasma excitation by a fast incident electron. Our treatment differs from that of Pines,[18] in that we use first-order time-dependent perturbation theory. Taking the Hamiltonian for the metal plus incident electron as $H+p^2/2m+H_{\text{int}}$, where H is the Hamiltonian for the metal alone and p is the momentum of the incident electron, we apply first-order perturbation theory to the interaction term $H_{\text{int}}=-e\varphi(\mathbf{x})$. Here $\varphi(\mathbf{x})$ is the electrostatic potential set up by the ions and electrons of the metal, evaluated at the position of the incident electron. The potential is determined from Poisson's equation, $\nabla^2\varphi(\mathbf{x})=4\pi e\rho(\mathbf{x})$, where $-e\rho(\mathbf{x})$ is the charge density in the metal. Expanding $\rho(\mathbf{x})$ in the Fourier series $\rho(\mathbf{x})=\sum_{\mathbf{k}}\rho_{\mathbf{k}}e^{-i\mathbf{k}\cdot\mathbf{x}}$ gives

$$\phi(\mathbf{x})=-4\pi e\sum_{\mathbf{k}}\frac{\rho_{\mathbf{k}}}{k^2}e^{-i\mathbf{k}\cdot\mathbf{x}}.$$

This makes possible the separation of $H_{\text{int}}=H'+H''$ into the long-range part,

$$H'=4\pi e^2\sum_{k<k_c}\frac{\rho_{\mathbf{k}}}{k^2}e^{-i\mathbf{k}\cdot\mathbf{x}},$$

and the short-range part,

$$H''=4\pi e^2\sum_{k>k_c}\frac{\rho_{\mathbf{k}}}{k^2}e^{-i\mathbf{k}\cdot\mathbf{x}}.$$

$\hbar k_c$ is the Bohm-Pines cut-off momentum. We leave the short-range part to the next section and concentrate for the present on the long-range interaction. For $k<k_c$, the electron density Fourier coefficients are, in terms of the coordinates $\mathbf{x}_i$ of the electrons participating in the plasma oscillations, $\rho_{\mathbf{k}}=V^{-1}\sum_i e^{i\mathbf{k}\cdot\mathbf{x}_i}=\rho_{\mathbf{k}}^{(1)}+i\rho_{\mathbf{k}}^{(2)}$, where $\rho_{\mathbf{k}}^{(1)}=V^{-1}\sum_i\cos(\mathbf{k}\cdot\mathbf{x}_i)$, $\rho_{\mathbf{k}}^{(2)}=V^{-1}\sum_i\sin(\mathbf{k}\cdot\mathbf{x}_i)$, and V is the volume of quantization. Here we are neglecting the contributions to $\rho_{\mathbf{k}}$ from the lattice vibrations.

Now, according to the discussion at the beginning of this section, the $\rho_{\mathbf{k}}$ oscillate harmonically, for small k. Although this is rigorously true only in the limit of infinitesimally small k, Bohm and Pines[5] have shown for the free-electron gas that the harmonic behavior exists approximately for all $k<k_c$. We assume here that this is true also in the more general case, and do not expect any appreciable error to arise from this approximation. The harmonic oscillator matrix elements of $\rho_{\mathbf{k}}$, which are needed for the perturbation calculation, can be found most easily from those for $\rho_{\mathbf{k}}^{(1)}$ and $\rho_{\mathbf{k}}^{(2)}$. In general, the matrix element, between the ground state and first excited state, of a real variable which oscillates harmonically is $(\Delta E/2K)^{\frac{1}{2}}$, where $\Delta E=\hbar\omega$, the energy of excitation, or simply the eigenloss, and K is the spring constant of the oscillator. The latter is easily determined from the total electrostatic potential energy in the metal, which is, aside from constant self-energy terms,

$$\begin{aligned}&\tfrac{1}{2}\int\varphi(\mathbf{x})[-e\rho(\mathbf{x})]d^3x\\&=\tfrac{1}{2}\cdot4\pi e^2\sum_{\mathbf{k}}\frac{1}{k^2}\rho_{\mathbf{k}}\int e^{-i\mathbf{k}\cdot\mathbf{x}}\rho(\mathbf{x})d^3x\\&=\tfrac{1}{2}\cdot4\pi e^2V\sum_{\mathbf{k}}\frac{|\rho_{\mathbf{k}}|^2}{k^2}=\tfrac{1}{2}\cdot8\pi e^2V\sum_{k_z>0}\frac{1}{k^2}(\rho_{\mathbf{k}}^{(1)2}+\rho_{\mathbf{k}}^{(2)2}).\end{aligned}$$

Therefore the spring constant for the oscillators belonging to $\rho_{\mathbf{k}}^{(1)}$ and $\rho_{\mathbf{k}}^{(2)}$ is $K=8\pi e^2V/k^2$, and the matrix element for excitation of these oscillators out of their ground states is $k(\Delta E/16\pi e^2V)^{\frac{1}{2}}$. From this result, it readily follows that the square of the matrix element of H' for the excitation of a plasma quantum of momentum $\hbar\mathbf{k}$, accompanied by recoil scattering of the incident electron, is

$$|H_{\mathbf{k}}'|^2=2\pi e^2\Delta E/Vk^2. \tag{5}$$

[18] See reference 5, p. 633.

In calculating the density of states, the kinetic energy of the fast incident electron predominates and the variation of the plasma energy with state may be neglected. Thus one finds

$$\rho(E)=Vmpd\Omega/h^3, \tag{6}$$

where p is the momentum of the incident electron and $d\Omega$ is the differential solid angle into which it is scattered. From (5) and (6), and first-order perturbation theory, the rate of inelastic scattering is

$$\frac{2\pi}{\hbar}\rho(E)\,|H_{\mathbf{k}}'|^2=\frac{p}{m}\cdot\frac{d\Omega}{2\pi a_0}\cdot\frac{m\Delta E}{(\hbar k)^2}. \tag{7}$$

Multiplication of Eq. (7) by the transit time for passage through a foil of thickness t gives for the probability of scattering into $d\Omega$ the expression $td(1/\lambda)$, where $d(1/\lambda)=(d\Omega/2\pi a_0)[m\Delta E/(\hbar k)^2]$ is the differential inverse mean free path. With the help of Fig. 1, which illustrates the restrictions imposed by energy-momentum conservation for small angles of scattering, one finds

$$(\hbar k)^2=(\Delta p)^2+p^2\theta^2=p^2[(\Delta p/p)^2+\theta^2]=p^2(\theta_E{}^2+\theta^2),$$

where θ is the angle of scattering and $\theta_E=\Delta p/p=\Delta E/2E$. Thus,

$$d(1/\lambda)=\left(\frac{d\Omega}{2\pi a_0}\right)\left(\frac{\theta_E}{\theta_E{}^2+\theta^2}\right). \tag{8}$$

Since the long-range scattering vanishes for $\theta>\hbar k_c/p=\theta_{cE}\gg\theta_E$, the total inverse mean free path is $1/\lambda=(\theta_E/a_0)\ln(\theta_{cE}/\theta_E)$. Hence the mean free path itself is

$$\lambda=\frac{a_0}{\theta_E\ln\left(\dfrac{\theta_{cE}}{\theta_E}\right)}=\frac{2a_0E}{\Delta E\ln\left[\dfrac{\hbar k_c}{\Delta E}\left(\dfrac{2E}{m}\right)^{\frac{1}{2}}\right]}. \tag{9}$$

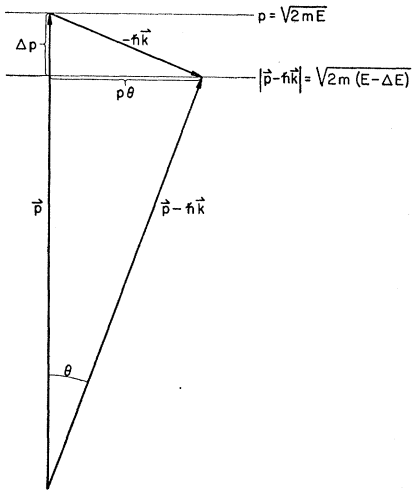

FIG. 1. Energy-momentum conservation for inelastic electron scattering from excitation of plasma quantum of momentum $\hbar\mathbf{k}$ and energy ΔE.

Equation (9) provides a check on our Eq. (8), and agrees, for the free-electron case of $\Delta E=\hbar(4\pi ne^2/m)^{\frac{1}{2}}$, with Pines'[5] equation (49), which was derived by another method. Equation (9) extends Pines' formula to cases more general than that of the free-electron gas.

III. ONE-ELECTRON THEORY

In addition to the long-range collective contribution to the inelastic electron scattering, there is also a short-range one-electron contribution. To avoid the complications of the band structure of real metals, we limit ourselves to the idealized model of the free-electron gas. Our purpose is (1) to give a qualitative treatment of the short-wavelength cutoff, and (2) to demonstrate that treating the long-range interaction also by one-electron theory, instead of by Bohm-Pines theory, gives erroneous results in disagreement with experiment.

The short-range interaction of N individual electrons with the incident electron is described by

$$H''=\frac{4\pi e^2}{V}\sum_{k>k_c}\frac{1}{k^2}\sum_i e^{i\mathbf{k}\cdot(\mathbf{x}_i-\mathbf{x})}. \tag{10}$$

Now the operator $\sum_i e^{i\mathbf{k}\cdot\mathbf{x}_i}$ converts the Slater determinant representing the unperturbed Fermi sea into $Nv(k/k_0)$ Slater determinants, where

$$v\left(\frac{k}{k_0}\right)=\frac{3}{4}\frac{k}{k_0}\left(1-\frac{k^2}{12k_0{}^2}\right)$$

is $3/4\pi$ times the volume of the shaded portion of the unit sphere shown in Fig. 2, and k_0 is the Fermi wave number. These $Nv(k/k_0)$ Slater determinants form an orthonormal set and represent excited states of the electron gas. Therefore the sum of the squared matrix elements associated with an incident electron recoil of $-\hbar\mathbf{k}$ is

$$\sum_{\text{states}}|H_{\mathbf{k}}''|^2=\frac{16e^4k_0{}^3}{3Vk^4}v(k/k_0)$$
$$=\frac{16e^4\hbar^2k_0}{3Vp^2}\cdot\frac{\theta_{0E}{}^2}{\theta^4}v(\theta/\theta_{0E}), \tag{11}$$

where we have substituted $N/V=k_0{}^3/3\pi^2$, and have introduced the parameter $\theta_{0E}=\hbar k_0/p$ and the angle of scattering $\theta=\hbar k/p$. A calculation similar to that of the preceding section yields for the short-range differential inverse mean free path:

$$d\left(\frac{1}{\lambda_{\text{s.r.}}}\right)=\frac{4}{3\pi^2}\cdot\frac{Ry\,k_0}{E}\cdot\frac{\theta_{0E}{}^2}{\theta^4}v(\theta/\theta_{0E})d\Omega. \tag{12}$$

It is interesting to compare this result with that of Sec. II for the long-range collective interaction. For $\theta/\theta_{0E}\leq 1$, $v(\theta/\theta_{0E})\cong\frac{3}{4}(\theta/\theta_{0E})$. Hence the short-range scattering varies as the inverse cube, while the long-range scattering varies only as the inverse square of the

angle. Consequently the curves representing these two scattering intensities as a function of angle will intersect one another. At large angles the short-range curve correctly determines the intensity of inelastic scattering, while at small angles the intensity of scattering is determined by the long-range curve. Therefore the intersection of the two curves gives roughly the cutoff in wave number which separates the collective from the one-electron phenomena. To determine this cutoff, we put $\theta=\theta_{cE}$, where

$$\theta_{cE}/\theta_{0E}=k_c/k_0=\beta,$$

and equate (12) to (8). Solving for β, we obtain

$$\beta=(4k_0a_0/\pi)(Ry/\Delta E). \tag{13}$$

Substituting the free-electron gas values of

$$k_0a_0=1.917/r_s \quad \text{and} \quad \Delta E=(46.9/r_s^2)\ \text{ev},$$

where $r_s=(3V/4\pi Na_0^3)^{\frac{1}{3}}$, we find

$$\beta=0.706\sqrt{r_s}. \tag{14}$$

It is interesting to note that (14) gives a cut-off ratio about twice that calculated by Pines,[5] who determines β by minimizing the expectation value of the total Hamiltonian. The apparent discrepancy here disappears when it is realized that we have not strictly determined the cutoff for collective oscillation, but rather an *effective cutoff* for Eq. (8). Even for wavelengths somewhat too short for collective oscillations to be sustained there may still be sufficient correlation among the electrons to yield (8). As still shorter wavelengths are considered, these correlations should gradually fade out, the more-or-less sharp eigenloss should become smeared out over a wide energy interval, and finally the scattering should be described correctly by the one-electron formula (12). The exact nature of this transition remains a subject for future investigation. For the time being, we satisfy ourselves with the following admittedly crude approximation: (1) For $\theta\leq\theta_{cE}$, (12) holds without modification; (2) for angles larger than θ_{cE}, there is *no eigenloss* scattering. The actual value of the cutoff, as we shall see, can be deduced from the experimental results. In any case, our discussion of the angular dependence will be independent of it, since we shall be dealing mainly with angles smaller than the cut-off angle.

To conclude this section, we wish to demonstrate that treating the long-range interaction by one-electron theory instead of by Bohm-Pines theory would result in disagreement with experiment, in several respects. Here we assume that our conclusions, based on the free-electron gas, because of their qualitative nature, will carry over to the case of a real metal.

First of all, the most obvious shortcoming of the one-electron theory is that it does not yield the eigenlosses, but instead a smeared-out distribution in energy between zero and $(\hbar^2/2m)(k^2+2kk_0)$, for inelastic scattering at angle $\theta=\hbar k/p$. In addition to this difficulty is

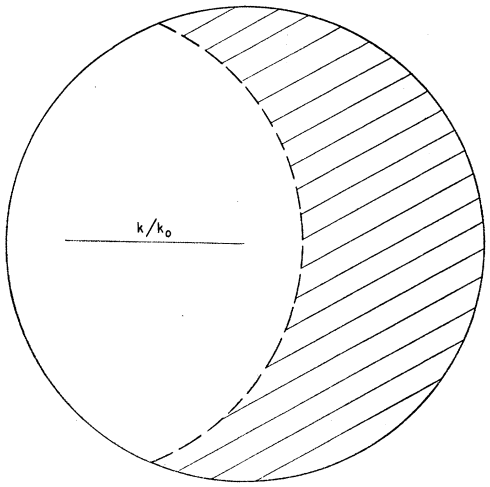

FIG. 2. Fraction of the Fermi sea susceptible to one-electron excitation.

the insufficiency in the amount of energy lost in the scattering process. Even at the relatively large angle of $\frac{1}{2}\theta_{0E}$ the maximum energy loss is only five-fourths the Fermi energy, which is still generally smaller than the eigenloss. At smaller angles, which account for the bulk of the scattering, the energy loss predicted on the one-electron theory is very much smaller than that experimentally observed.

Aside from the magnitude of the energy loss, the total intensity of inelastic scattering on the basis of one-electron theory alone is an additional indication of inadequacy of the latter theory. Integrating (12) over all angles $\theta\geq\theta_{cE}=\beta\theta_{0E}$, one easily finds for the total inverse mean free path:

$$\frac{1}{\lambda_{s.r.}}=\frac{2k_0}{\pi}\cdot\frac{Ry}{E}\cdot\left(\frac{1}{\beta}+\frac{\beta}{12}-\frac{1}{2}\right).$$

This expression clearly diverges when the cutoff is allowed to pass to zero. This divergence can be directly traced to a too-large expectation value of the operator $|\rho_k|^2$, resulting from appreciable probability in the ground state for excessively large values of this operator. Now it is just these large values which would unduly raise the potential energy and which do not actually occur in the true many-electron ground state of the system. The long-range positional correlations which prevent the electrons from assuming configurations corresponding to large density fluctuations are ignored by the free electron theory. By taking the correlations into account, the Bohm-Pines theory more correctly describes both the stationary states and the scattering properties of the electron gas.

Since the divergence in the inelastic scattering intensity predicted on the basis of the one-electron theory arises from very strong scattering at very small angles with very small loss in energy, it might be claimed that the mean free path is not measurable and that the

stopping power is a more appropriate description of the scattering. We therefore turn for the moment to the calculation of the stopping power of a free electron gas for fast electrons. In every collision in which an electron of momentum $\hbar k_1$ is excited above the Fermi sea by the transfer of momentum $\hbar k$, the energy $(\hbar^2/2m)\times(k^2+2\mathbf{k}\cdot\mathbf{k}_1)$ is absorbed from the incident electron. By summing over all k_1's susceptible of excitation (see Fig. 2) we find that the energy loss per unit path length resulting from scattering into the solid angle $d\Omega$ is given simply by multiplying the short-range differential inverse mean free path of Eq. (12) by the average energy of excitation $\hbar^2k^2/2mv(k/k_0)$. Thus the differential short-range stopping power is

$$dS_{\text{s.r.}}=\frac{\Delta E\theta_E}{2\pi a_0}\cdot\frac{d\Omega}{\sin^2\theta}, \tag{15}$$

where, in place of the approximation $\hbar k=p\theta$, we have used the exact relation $\hbar k=p\sin\theta$, correct for large angles as well as small. The expressions $k_0^3/3\pi^2=n$, $4\pi\hbar^2ne^2/m=(\Delta E)^2$, and $\Delta E/2E=\theta_E$ have also been employed in arriving at (15). It is interesting to note that $dS_{\text{s.r.}}$ exactly equals $dS_{\text{l.r.}}=\Delta E d(1/\lambda)$ for angles $\theta\gg\theta_E$. Because of this circumstance the total stopping power of the Fermi gas is insensitive to the choice in the value of the cutoff used for the calculation. Integrating (15) over all $\theta_{cE}<\theta\leqslant\pi/2$, we find for the total short-range stopping power:

$$S_{\text{s.r.}}=\frac{\Delta E\theta_E}{a_0}\int_{\theta_{cE}}^{\pi/2}\frac{d\theta}{\sin\theta}=\frac{\Delta E\theta_E}{a_0}\ln(\cot\theta_{cE}/2)$$
$$\approx\frac{\Delta E\theta_E}{a_0}\ln\left(\frac{2}{\theta_{cE}}\right). \tag{16}$$

Adding this to the long-range contribution,

$$S_{\text{l.r.}}=\Delta E/\lambda=\frac{\Delta E\theta_E}{a_0}\ln\left(\frac{\theta_{cE}}{\theta_E}\right),$$

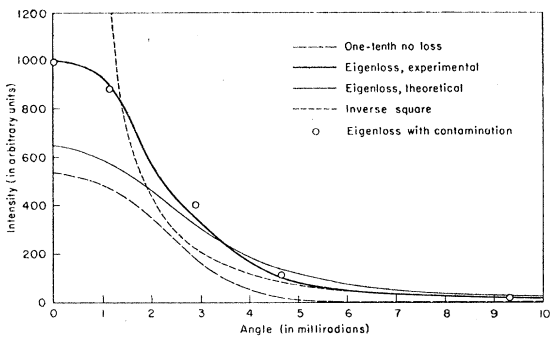

FIG. 3. Plot of scattered intensity *vs* angle for 20-kev electrons passing through thin gold foil [single crystal, (002) direction].

the total stopping power is

$$S=S_{\text{l.r.}}+S_{\text{s.r.}}=\frac{\Delta E\theta_E}{a_0}\left[\ln\left(\frac{\theta_{cE}}{\theta_E}\right)+\ln\left(\frac{2}{\theta_{cE}}\right)\right]$$
$$=\frac{\Delta E\theta_E}{a_0}\ln\left(\frac{2}{\theta_E}\right). \tag{17}$$

Since the arguments of the logarithms are both proportional to $\sqrt{E}$, the long- and short-range contributions will be practically equal in all cases of relatively high energy (compared to ΔE).

Now if we were to use only the one-electron theory without the Bohm-Pines theory to supplement it, we would be forced to allow θ_{cE} to go to zero in (16), thus obtaining an infinite stopping power—in manifest disagreement with experiment.[19] Because of this and the other reasons listed above, there seems to be no alternative to the Bohm-Pines theory for small-angle intraband transitions. The foregoing discussion does not, however, apply to interband transitions, and such excitations undoubtedly account for many of the eigenlosses observed in metals. We assume, however, that for the 24-ev eigenloss in gold this is not the case and proceed in the next section to compare Eq. (8) with the angular distribution found by Marton, Simpson, and McCraw.

IV. COMPARISON WITH EXPERIMENT

The experimental results of Marton, Simpson, and McCraw are shown on Fig. 3. The heavy dashed line represents one-tenth the intensity of the no-loss elastic scattering, while the heavy solid line shows the angular dependence of the 24-ev eigenloss inelastic scattering. This latter angular dependence fits an inverse square curve (i.e., θ^{-2}), for angles greater than about seven milliradians. (The inverse square falloff extends to about twelve milliradians, at which point the distribution is affected by wide-angle screened-Coulomb atomic scattering due to lattice impurities and irregularities. By dealing mainly with smaller angles we are able to ignore this additional complication in the present work.) The inverse square behavior is predicted by Eq. (8) and its appearance at the larger angles encourages one to attempt to account for the course of the entire eigenloss curve on the basis of this formula. The deviation of the observed eigenloss distribution at smaller angles can immediately be attributed to the spread in the no-loss beam, in turn due to elastic scattering by the lattice waves. Without further modification, Eq. (8) describes only the case of a precisely collimated no-loss beam.

To describe the physically more realistic case, let us choose coordinates so that the front surface of the metal

[19] For other discussions of the stopping power of the conductivity electrons see: H. A. Kramers, Physica **13**, 401 (1947); Aage Bohr, Kgl. Danske Videnskab. Selskab, Mat.-fys. Medd. **24**, 19 (1948); and David Pines, Phys. Rev. **92**, 626 (1953).

foil, exposed to the normally incident fast electron beam, lies in the $x-y$ plane, with $z=0$. The back surface is then specified by $z=t$, where t is the thickness. (See Sec. II for notation.) At any depth $0\leq z\leq t$ within the metal, let $I(\boldsymbol{\theta},z)$ and $J(\boldsymbol{\theta},z)$ represent the no-loss and eigenloss distributions, respectively, where $\boldsymbol{\theta}$ is a two-dimensional vector lying in the $x-y$ plane. Its components, θ_x and θ_y, are the projections of the unit propagation vector, and its magnitude is simply θ, the angle of scattering. Making the further definitions, $\Lambda=$net mean free path for all inelastic processes, $f(\boldsymbol{\theta})=d(1/\lambda)/d\Omega$, eigenloss scattering coefficient, and $g(\boldsymbol{\theta})=$corresponding elastic scattering coefficient, we can write the following equations[20]:

$$\frac{dI(\boldsymbol{\theta},z)}{dz}=\int d^2\boldsymbol{\theta}'g(\boldsymbol{\theta}-\boldsymbol{\theta}')I(\boldsymbol{\theta}',z)-\frac{1}{\Lambda}I(\boldsymbol{\theta},z), \tag{18}$$

$$\frac{dJ(\boldsymbol{\theta},z)}{dz}=\int d^2\boldsymbol{\theta}'g(\boldsymbol{\theta}-\boldsymbol{\theta}')J(\boldsymbol{\theta}',z)-\frac{1}{\Lambda}J(\boldsymbol{\theta},z)+\int d^2\boldsymbol{\theta}'f(\boldsymbol{\theta}-\boldsymbol{\theta}')I(\boldsymbol{\theta}',z). \tag{19}$$

Here we regard $g(\boldsymbol{\theta})$ as having a negative Dirac delta function-like behavior at $\boldsymbol{\theta}=0$, such that $\int d^2\boldsymbol{\theta}g(\boldsymbol{\theta})=0$. Introducing the Green's function $G(\boldsymbol{\theta},z)$ as the solution of Eq. (18) with the boundary condition

$$G(\boldsymbol{\theta},z)\,|_{z=0}=\delta^{(2)}(\boldsymbol{\theta}),$$

we find

$$I(\boldsymbol{\theta},z)=I_iG(\boldsymbol{\theta},z) \tag{20}$$

and

$$J(\boldsymbol{\theta},z)=I_i\int_0^z dz'\int d^2\boldsymbol{\theta}''\times\int d^2\boldsymbol{\theta}'G(\boldsymbol{\theta}-\boldsymbol{\theta}'',z-z')f(\boldsymbol{\theta}''-\boldsymbol{\theta}')G(\boldsymbol{\theta}',z'), \tag{21}$$

where

$$I_i=\int I(\boldsymbol{\theta},0)d^2\boldsymbol{\theta}$$

is the total incident no-loss intensity. We have assumed the incident beam to be precisely collimated, which corresponds closely to the actual experimental setup.

Although Eqs. (20) and (21) give a complete description of the no-loss and eigenloss at every point in the metal they can be compared with experiment only at $z=t$, where the beams emerge from the back surface of the foil and are subject to measurement. Before specializing (20) and (21) to $z=t$, however, let us first note that it is possible greatly to simplify (21) by reducing the double convolution to a single convolution. This can be seen by eliminating $\boldsymbol{\theta}''$ in terms of the variable $\boldsymbol{\psi}=-\boldsymbol{\theta}''+\boldsymbol{\theta}+\boldsymbol{\theta}'$. Then

$$\int\int d^2\boldsymbol{\theta}''d^2\boldsymbol{\theta}'G(\boldsymbol{\theta}-\boldsymbol{\theta}'',z-z')f(\boldsymbol{\theta}''-\boldsymbol{\theta}')G(\boldsymbol{\theta}',z')=\int d^2\boldsymbol{\psi}f(\boldsymbol{\theta}-\boldsymbol{\psi})\int d^2\boldsymbol{\theta}'G(\boldsymbol{\psi}-\boldsymbol{\theta}',z-z')G(\boldsymbol{\theta}',z').$$

From the nature of the Green's function,

$$\int d^2\boldsymbol{\theta}'G(\boldsymbol{\psi}-\boldsymbol{\theta}',z-z')G(\boldsymbol{\theta}',z')=G(\boldsymbol{\psi},z).$$

Therefore, using (20), (21) reduces to

$$J(\boldsymbol{\theta},z)=z\int d^2\boldsymbol{\theta}'f(\boldsymbol{\theta}-\boldsymbol{\theta}')I(\boldsymbol{\theta}',z). \tag{22}$$

We now put $z=t$, represent the outcoming distributions by simply $I(\theta)$ and $J(\theta)$, and substitute for $f(\boldsymbol{\theta}-\boldsymbol{\theta}')$. Taking advantage of the symmetry of the no-loss distribution about $\boldsymbol{\theta}'=0$ in order carry out the integration around circles of radius θ', we obtain

$$J(\theta)=K\int_0^{\theta_M}\frac{\theta'I(\theta')d\theta'}{[(\theta'^2-\theta^2+\theta_E^2)^2+4\theta^2\theta_E^2]^{\frac{1}{2}}}. \tag{23}$$

Here $K=t\theta_E/a_0$, θ_M is such that for $\theta'\geq\theta_M$, $I(\theta')$ is essentially zero, and the equation holds only for $\theta\leq\theta_{cE}-\theta_M$. It should be noted that (23) predicts an inverse square behavior, regardless of the particular form of the no-loss curve, provided θ is large compared to θ_M. In this case, the denominator can be replaced by θ^2 and taken in front of the integral sign, resulting in

$$J(\theta)\approx KI_0/2\pi\theta^2, \tag{24}$$

where $I_0=\int_0^{\theta_M}2\pi\theta I(\theta)d\theta$ is the total no-loss intensity emerging from the foil.

Corresponding to (21), there is an equation for $I(\theta)$ itself in terms of the Green's function $G(\boldsymbol{\theta},t)$. Although in principle it is possible to calculate this Green's function from the basic theory of lattice vibrations, we do not do so here. Instead, we take $I(\theta)$ as given by the experimental data. Proceeding, therefore, to calculate the eigenloss distribution from Eq. (23), we need to know the value of the numerical parameter K, which depends on the thickness of the target foil. The latter can be estimated independently from the evaporation method used to prepare the foil. It is difficult in this way, however, to obtain a value for the thickness which can be relied upon to better than a factor of two. Therefore, although the experimenters have assigned the nominal thickness of 100 A to the gold foil upon which the present analysis is based, we prefer here to determine t by normalizing the total eigenloss intensity calculated on the basis of $J(\theta)$ so that it agrees with the

[20] In restricting our attention to the intensities, we neglect any coherence of the lattice or plasma waves which could lead to constructive or destructive interference between waves excited at different points in the metal. Because of the shortness of the phonon mean free path at room temperature and the smallness of the plasma group velocity this can be expected to be a good approximation.

total measured eigenloss intensity. More precisely, we carry out the normalization for the quantity $J_N=\int_0^{\theta_N} 2\pi\theta J(\theta)d\theta$, where θ_N is chosen small enough that (23) remains valid, but sufficiently large compared to θ_M that simplifying approximations can be employed. Under these conditions it is easily established that

$$K\approx\frac{J_N}{I_0\ln(\theta_N/\theta_E)}.$$

In the experiment carried out by Marton and co-workers, 20-kev electrons were employed. Therefore $\theta_E=\Delta E/2E=0.6$ milliradian. Concerning the choice of θ_N, we are confronted by the fact that the value of θ_{cE} is not known. As long, however, as we remain in the inverse square region we can be confident that we have not violated the condition $\theta_N<\theta_{cE}-\theta_M$, which is essential to the validity of (23) and, hence, (24). The actual value chosen was $\theta_N=11.64$ milliradians, corresponding to $\ln(\theta_N/\theta_E)=2.96$. Numerical integration of the two experimental curves separately then yields $K=0.0911$, corresponding to a thickness of 80.2 A. Equation (23) can now be numerically integrated for various values of θ. The results are presented by the thin line in Fig. 3.

Although the theoretical eigenloss curve of Fig. 3 successfully portrays the general trend of the experimental curve as it drops smoothly from relatively high values at small angles to a long weak tail at larger angles, there are two significant discrepancies between the theoretical and experimental curves. First, the theoretical intensity at small angles falls short by a considerable amount of accounting for the observed intensity. Second, the theoretical tail is somewhat stronger than the observed. A natural explanation of the first discrepancy, which is perhaps the more striking one, results when one realizes that it is just at these small angles that the intensity of the no-loss beam is very high. (See Fig. 3.) In this type of experiment it is technically very difficult to measure with extreme precision both angle and energy simultaneously. To achieve high angular resolution Marton and co-workers were forced to sacrifice energy resolution to the extent that at angles less than 4 milliradians the eigenloss beam was swamped by the intense no-loss beam, and could not be resolved. An examination of the cartograph for the case "100 A Au single crystal (002 direction)"[21] suggests that the no-loss beam may make as much as a 10% "contamination" contribution to the "eigenloss" intensity.

If this contamination effect is accepted, it is no longer possible to normalize $J(\theta)$ to integrated intensity. The value of K must be determined rather by comparing the inverse square tails of the calculated and observed eigenloss intensities at large angles, where $I(\theta)$ vanishes and there is no contamination. Fitting the two curves over the interval seven to twelve milliradians yields $K=0.0619$, corresponding to a thickness of 54.5 A. The theoretical intensity at zero angle on the basis of this value of K is lowered to 440, compared to an experimental value of 1000 for $J(0)$ and 5400 for $I(0)$ in the same units. Therefore 560, or more than half of the "eigenloss" intensity at zero angle, must come from the no-loss beam. This corresponds to a "contamination coefficient" of $560/5400=0.1034$, or about ten percent. Now using the same value of contamination coefficient for all angles, one adds 0.1034 $I(\theta)$ to $J(\theta)$, evaluated from (23) with $K=0.0619$, and compares the sum with the observed "eigenloss" intensity. The results are shown in the form of several points plotted on Fig. 3. The procedure is such as to give automatically exact agreement between theoretical and experiment values for very small and very large angles. Intermediate angles do, however, provide a test, and the good agreement in this range seems to substantiate this interpretation of the data.

We conclude this section with a brief numerical treatment of the short-wavelength cutoff, a discussion of which has already been given in Sec. III. From that discussion we should expect zero eigenloss intensity for angles $\theta>\theta_M'=\theta_{cE}+\theta_M$. This fact should thus provide a means of estimating θ_{cE}. The actual value of θ_{cE} could easily be obtained by integrating the eigenloss intensity, obtaining numerically the quantity

$$J_0=\int_0^{\theta_M'} 2\pi\theta J(\theta)d\theta.$$

Since it is easily established that $J_0=(t/\lambda)I_0$, one could solve for

$$\lambda=\frac{a_0}{\theta_E\ln(\theta_{cE}/\theta_E)}.$$

From this expression θ_{cE} would then be easily obtained and from θ_{cE}, in turn, the Bohm-Pines cut-off parameters, k_c and β.

Unfortunately, the experimental eigenloss curve does not drop to zero for any value of θ, and the procedure outlined above cannot be carried through. As mentioned above, the inverse square falloff is appreciably augmented, at angles greater than twelve milliradians, by wide-angle atomic scattering. At still greater angles another contributor is the one-electron short-range scattering dealt with in Sec. III. Because of the finite resolving power of the detector, this one-electron scattering can contribute to the "eigenloss" intensity despite its diffuseness in energy. This effect could, in principle, be eliminated by using a detector sharply adjusted to the eigenloss. In practice, however, it may be difficult to obtain the necessary extreme energy resolution. The one-electron scattering is no doubt the principal contributor in the present case at angles well above the inverse square region, and prevents a unique determination of the cutoff from the present data. If we

[21] Figure 2 of reference 12.

nevertheless arbitrarily set $\theta_M'=2\theta_N$ and assume that there is no long-range scattering at angles greater than this, we find $J_0/I_0=0.214$, where the contamination from I_0 has been subtracted from J_0. With the previous value for the thickness, $t=54.5$ A, this yields $\lambda=255$ A, or $\theta_{cE}=19.1$ milliradians. Since $\theta_{cE}=\hbar kc/p$ by definition, we find $k_c=0.733a_0^{-1}$. For the free electron gas it is generally convenient to compare k_c with the Fermi momentum, k_0. In the case of gold, however, the electrons are far from free and the definition of k_0 is ambiguous. If we take it as defined by $k_0=1.917(r_sa_0)^{-1}$, where r_s is determined by its free-electron formula (see Sec. III), we find $r_s=3.05$, and $k_0=0.629a_0^{-1}$, assuming one electron per atom. Including the d-electrons to give a total of eleven electrons per gold atom yields $r_s=1.371$, $k_0=1.398a_0^{-1}$. The ratios $\beta=k_c/k_0$ calculated with these values of k_0 and $\beta=1.165$ and $\beta=0.525$, in order of magnitude agreement with the values $\beta=1.232$ and $\beta=0.826$ calculated from Eq. (14) of Sec. III. Because of the complications caused by the short-range scattering and the effects of binding, the numerical results in this paragraph should not be regarded seriously. They have been obtained only to illustrate the method which can be followed in a more ideal case.

V. SUMMARY

The above work shows that the experimental angular dependence of the 24-ev characteristic energy loss in gold is consistent with a simple Bohm-Pines approach, provided that a correction is made for finite energy resolution. It may be that the theory of band excitation could yield similar agreement; however, this could be established only on the basis of a detailed energy band calculation. In any case, there are general criteria based on optical data, which are able in principle to decide, for any given characteristic energy loss, between the two alternative mechanisms. Furthermore, there are certain phenomena, such as the slowing down of electrons, to which both mechanisms for the excitation of the electrons of the metal contribute. In the analysis of these phenomena a collective treatment is indispensable.

ACKNOWLEDGMENTS

It is a pleasure to thank Dr. Marton and his coworkers for many interesting discussions and for the communication of their results in advance of publication. The author is in addition indebted to Dr. U. Fano, Dr. H. Mendlowitz, and Professor David Pines for valuable suggestions and comments.

PHYSICAL REVIEW VOLUME 101, NUMBER 2 JANUARY 15, 1956

Infrared Absorption of Indium Antimonide*

EUGENE BLOUNT, JOSEPH CALLAWAY,† MORREL COHEN, WILLIAM DUMKE, AND JAMES PHILLIPS
Chicago Midway Laboratories, The University of Chicago, Chicago, Illinois

(Received September 12, 1955)

Infrared absorption in InSb near the absorption edge has been interpreted as the superposition of two indirect transitions requiring phonons of 100° and 30°, the former transition involving the smaller electronic energy gap. The first transition is consistent with a band scheme having electrons at the center of the zone and holes either at the corner of the zone or about halfway along the [1,1,1] line. The other transition may indicate a second hole with an energy gap about 0.025 ev larger than that of the first.

THE theory of indirect transitions between valence and conduction bands proposed by Bardeen, Blatt, and Hall[1] and applied to germanium and silicon by Macfarlane and Roberts[2] and Fan, Shepard, and Spitzer,[3] has been applied to the infrared absorption of indium antimonide. Measurements of the absorption coefficient of indium antimonide[4,5] (shown in Fig. 1) reveal that close to the absorption edge, the absorption coefficient, K, conforms reasonably well to the following formula:

$$K=\frac{A}{e^{\theta/T}-1}[(\hbar\omega-E_g+k\theta)^2+e^{\theta/T}(\hbar\omega-E_g-k\theta)^2], \quad (1)$$

where E_g is the minimum separation between the valence and conduction bands (not vertical) and $k\theta$ is the energy of a phonon emitted or absorbed in the transition (k is the Boltzmann constant). Analysis of the measurements yields a value for θ of approximately 100° and

* Research supported by the United States Air Force through the Office of Scientific Research of the Air Research and Development Command.

† Permanent address, Department of Physics, University of Miami, Coral Gables, Florida.

[1] Bardeen, Blatt, and Hall, Proceedings of the Atlantic City Photoconductivity Conference, 1954 (John Wiley and Sons, Inc., New York, 1955).

[2] G. C. Macfarlane and V. Roberts, Phys. Rev. **97**, 1714 (1955); **98**, 1865 (1955).

[3] Fan, Shepard, and Spitzer, Proceedings of the Atlantic City Photoconductivity Conference, 1954 (John Wiley and Sons, Inc., New York, 1955).

[4] A. Goldberg (private communication).

[5] G. C. Macfarlane (private communication to S. W. Kurnick). We are indebted to Dr. Macfarlane for furnishing his unpublished data.